P1.5

PHOTOENHANCEMENT… OR PHOTODEPRESSION?... OF THE HYDROLYSIS OF NO_2: IMPLICATIONS FOR THE CHEMISTRY OF POLLUTED ATMOSPHERES

Kevin A. Ramazan, Dennis Syomin
and Barbara J. Finlayson-Pitts*
University of California, Irvine

1. INTRODUCTION

Nitrous acid (HONO) was first identified in ambient urban air in 1979 [*Perner and Platt,* 1979]. Since then, a number of atmospheric measurements have been made showing that HONO accumulates during the night, and undergoes photolysis in the early morning to produce a pulse of hydroxyl radicals (OH) [*Platt et al.,* 1980; *Winer and Biermann,* 1994; *Harrison et al.,* 1996; *Lammel and Cape,* 1996; *Lammel,* 1999; *Schiller et al.,* 2001; *Alicke et al.,* 2002; *Stutz et al.,* 2002]. HONO photolysis is believed to be a major source of OH in the early morning. [*Winer and Biermann,* 1994; *Harrison et al.,* 1996; *Alicke et al.,* 2002; *Stutz et al.,* 2002]. Both the OH and nitric oxide (NO) formed participate in reactions with volatile organic compounds (VOC) which lead to tropospheric O_3 formation, the principal component of photochemical smog [*Finlayson-Pitts and Pitts,* 2000]. Therefore, it is important to understand the sources and sinks of HONO, and the mechanism of its formation.

The major atmospheric source of HONO is believed to be the heterogeneous reaction of NO_2 with water. This hydrolysis of NO_2 is generally represented by (1):

$$2\ NO_2 + H_2O \xrightarrow{\text{surface}} HONO + HNO_{3(\text{surface})} \qquad (1)$$

It involves gas phase NO_2 reacting with water on surfaces, such as the walls of laboratory reactors, glass, concrete or foliage [*Wingen et al.,* 2002 (Paper No. P1.8)]. Reaction (1) has been studied extensively by reacting gas phase NO_2 in reaction chambers in the presence of water vapor [*Wayne and Yost,* 1952; *Caudle and Denbigh,* 1953; *Peters and Holman,* 1955; *Graham and Tyler,* 1972; *England and Corcoran,* 1974; *Sakamaki et al.,* 1983; *Pitts et al.,* 1984; *Akimoto et al.,* 1987; *Svensson et al.,* 1987; *Jenkin and Cox,* 1988; *Febo and Perrino,* 1991; *Mertes and Wahner,* 1995; *Kleffmann et al.,* 1998; *Goodman et al.,* 1999; *Cheung et al.,* 2000; *Finlayson-Pitts et al.,* 2002]. The mechanism of reaction (1) is currently poorly understood. In these NO_2 hydrolysis experiments, the HONO produced was measured in the gas phase, but gas phase HNO_3 was not detected [*England and Corcoran,* 1974; *Sakamaki et al.,* 1983; *Pitts,* 1984]. The HNO_3 is now known to remain adsorbed on the walls of the reaction chamber, and has been directly observed using transmission FTIR spectroscopy [*Barney and Finlayson-Pitts,* 2000; *Goodman et al.,* 2001]. One mechanism for (1), suggested many years ago, includes dinitrogen tetroxide (N_2O_4) as an intermediate [*Caudle and Denbigh,* 1953; *England and Corcoran,* 1974]. More recently this species has been observed on silica surfaces [*Goodman et al.,* 1999; *Barney and Finlayson-Pitts,* 2000]. This, and the additional detection of other species such as NO_2^+, has led Finlayson-Pitts and coworkers to propose a new mechanism [*Finlayson-Pitts et al.,* 2002]. A schematic diagram of the main points of this proposed mechanism is shown in Figure 1:

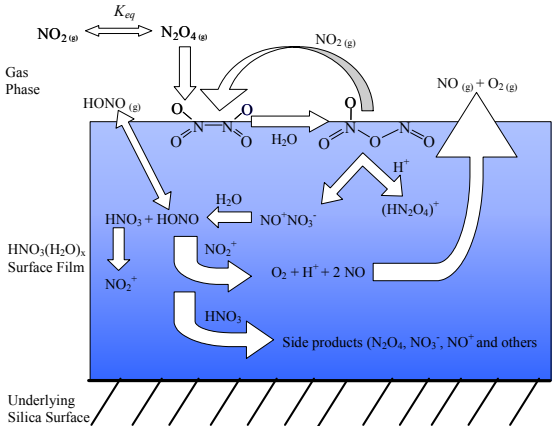

Figure 1. Reaction mechanism for NO_2 hydrolysis as proposed by Finlayson-Pitts *et al.* (2002).

In the proposed mechanism, gaseous N_2O_4, in equilibrium with NO_2, is taken up on the water film present on the surface. N_2O_4 isomerizes to the reactive species asymmetric N_2O_4 ($ONONO_2$). The asymmetric form of N_2O_4 then autoionizes to form the complex $NO^+NO_3^-$. This complex reacts with water to form HONO and HNO_3. In order for the mechanism to be first order in NO_2, as many previous studies report [*Sakamaki et al.,* 1983; *Pitts,* 1984; *Svensson et al.,* 1987; *Jenkin and Cox,* 1988; *Perrino et al.,* 1988; *Febo and Perrino,* 1991; *Wiesen et al.,* 1995; *Harrison and Collins,* 1998; *Kleffmann et al.,* 1998], a back reaction involving NO_2 reacting with asymmetric $ONONO_2$ must be faster than its reaction with water. Some of the HONO produced is released into the gas phase, while the remaining partakes in further chemistry at the surface to produce gaseous NO, O_2 and other side

* *Corresponding author address:* Barbara J. Finlayson-Pitts, Univ. of California, Irvine, Dept. of Chemistry, Irvine, CA 92697-2025; e-mail bjfinlay@uci.edu.

products. The HNO_3 stays adsorbed to the surface also leading to the production of various side products.

Akimoto and coworkers (1987), using a 6065 L smog chamber, showed that the HONO production by NO_2 hydrolysis in air is significantly enhanced in the presence of light ($\lambda > 290$ nm) [*Akimoto et al.,* 1987]. Nitrous acid formation was determined to be photoenhanced by the comparison of HONO concentration time-profiles measured using long path Fourier transform infrared spectroscopy (LP-FTIR) to model-predicted results. However, the mechanism of such a photoenhancement is not clear.

To determine the degree of photoenhancement, Akimoto *et al*. (1987), used a gas phase kinetics model that specified all the gas phase reactions occurring in the chamber. In order for the model to accurately predict the results in the cell, gas phase modeling data first had to be formulated for the heterogeneous NO_2 hydrolysis reaction in the dark. Akimoto *et al*. accomplished this by adding the following heterogeneous reactions to the gas phase model:

$$NO_2 + H_2O \rightarrow HONO \quad (2)$$

$$NO_2 + H_2O \rightarrow HNO_{3(wall)} \quad (3)$$

$$NO_2 + H_2O \rightarrow NO \quad (4)$$

$$NO_2 \rightarrow NO_{2(wall)} \quad (5)$$

By fitting these reactions to the experimental data, in both the dark and light experiments, Akimoto *et al.* determined the photoenhancement factor to be $\{(k_2'/k_2)-1\} = (6.8 \pm 2.5)k_p$ where k_2' is the rate constant of (2) in the presence of light and k_p is the photolysis rate constant of NO_2, which is included as a measure of light intensity.

In the present study, the rate of HONO formation is determined from NO_2 hydrolysis with varying concentrations of initial NO_2 (20 – 100 ppm) and relative humidities (20 – 80% RH) in the presence and absence of light (300 – 400 nm). Kinetics modeling is used to elucidate differences between experimental data and results expected based on the newly proposed mechanism of NO_2 hydrolysis.

2. EXPERIMENTAL METHODS

A cylindrical borosilicate glass long path cell (LPC) (150 mm i.d., 1 m base path, and 19.4 L volume) equipped with White optics [*White,* 1942] aligned and calibrated to a path length of 84 meters was used as a reaction vessel (Figure 2). The flanges and inner supports consist of anodized aluminum which is covered in a thin coating of halocarbon wax to minimize reactions with metal surfaces.

Concentrations of NO_2, HONO, and NO in the LPC were measured using FTIR (Mattson, Research Series) at 1 cm^{-1} resolution. Spectra were typically averaged over 64 scans, but when a faster sampling rate was required, they were averaged over 16 scans. NO_2, HONO, and NO were measured by the net absorbance of their peaks at 2917 cm^{-1}, 1263 cm^{-1}, and 1875 cm^{-1}, respectively. NO_2 and NO were calibrated in the LPC, while the HONO concentrations were calculated from an effective cross section of (3.7 ± 0.4) x 10^{-19} cm^2 $molecule^{-1}$ (base 10) [*Barney et al.,* 2001].

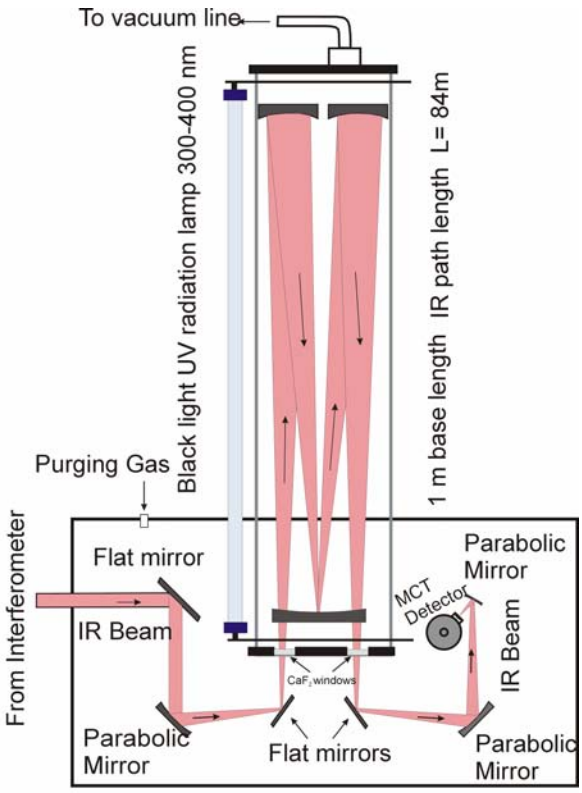

Figure 2. Diagram of the long path cell coupled to an FTIR spectrometer.

In each hydrolysis experiment, NO_2 was injected into the LPC in diluent nitrogen (N_2) (Oxygen Service Co., 99.999%) gas. NO_2 was synthesized by mixing NO (Matheson, 99%) with excess oxygen (O_2) (Oxygen Service Co., 99.993%) for ~ 2 hr. The NO_2 was then purified by condensing at 195 K and then pumping away the excess O_2. The LPC was filled to atmospheric pressure with the appropriate amount of humidified air from a collapsible Teflon chamber. Humidified air was added to a Teflon chamber by flowing N_2 gas through a bubbler filled with Nanopure® water (Barnstead, 18.2 MΩ cm) and mixing with dry N_2 to give the relative humidity desired. The use of a Teflon chamber provides a method of quickly bringing the cell to 1 atm. The HONO was allowed to build up in the dark for ~2 hr and then the photolysis lamps were switched on while continuously monitoring by FTIR. Irradiation (300-400 nm) entered the LPC through the borosilicate walls and was provided a Sylvania 350 black light (30 W, F30T8 / 350BL). All experiments were performed at room temperature.

Table 1. Chemical Reactions in Model

Reaction	Rate Constant (k^{298})[a] (cm^3 $molec^{-1}$ s^{-1} or s^{-1})	Reference
$2\ NO_2 \rightarrow N_2O_4$	2.85×10^{-14}	[*Atkinson et al.,* 2001]
$N_2O_4 \rightarrow 2\ NO_2$	1.23×10^{-05}	[*Atkinson et al.,* 2001]
$2\ NO_2 \rightarrow NO + NO_3$	4.62×10^{-28}	[*Tsang and Herron,* 1991]
$NO_3 + NO \rightarrow 2\ NO_2$	2.60×10^{-11}	[*DeMore et al.,* 1997]
$2\ NO_2 \rightarrow 2\ NO + O_2$	1.87×10^{-31}	[*Tsang and Herron,* 1991]
$NO_2 + NO_3 \rightarrow N_2O_5$	1.18×10^{-12}	[*DeMore et al.,* 2000]
$N_2O_5 \rightarrow NO_2 + NO_3$	5.75×10^{-02}	[*Atkinson et al.,* 2001]
$NO_2 + O(^3P) \rightarrow NO + O_2$	1.00×10^{-11}	[*DeMore et al.,* 2000]
$NO_2 + O(^3P) \rightarrow NO_3$	1.57×10^{-12}	[*DeMore et al.,* 1997]
$NO_2 + O_3 \rightarrow NO_3 + O_2$	3.20×10^{-17}	[*DeMore et al.,* 1997]
$NO_2 + OH \rightarrow HNO_3$	9.04×10^{-12}	[*DeMore et al.,* 2000]
$NO_2 + HO_2 \rightarrow HO_2NO_2$	1.39×10^{-12}	[*DeMore et al.,* 1997]
$NO_2 + H \rightarrow OH + NO$	1.30×10^{-10}	[*DeMore et al.,* 1997]
$NO + NO_2 \rightarrow N_2O_3$	7.29×10^{-15}	[*Atkinson et al.,* 2001]
$N_2O_3 \rightarrow NO + NO_2$	$3.76 \times 10^{+05}$	[*DeMore et al.,* 1997]
$NO + O(^3P) \rightarrow NO_2$	1.66×10^{-12}	[*DeMore et al.,* 2000]
$NO + O_3 \rightarrow NO_2 + O_2$	1.90×10^{-14}	[*DeMore et al.,* 2000]
$NO + OH \rightarrow HONO$	7.29×10^{-12}	[*Atkinson et al.,* 2001]
$NO + HO_2 \rightarrow OH + NO_2$	8.10×10^{-12}	[*DeMore et al.,* 1997]
$NO_3 + O(^3P) \rightarrow O_2 + NO_2$	1.00×10^{-11}	[*DeMore et al.,* 1997]
$NO_3 + OH \rightarrow HO_2 + NO_2$	2.00×10^{-11}	[*Atkinson et al.,* 2001]
$NO_3 + HO_2 \rightarrow OH + NO_2 + O_2$	4.00×10^{-12}	[*Atkinson et al.,* 2001]
$N_2O + O(^1D) \rightarrow N_2 + O_2$	4.90×10^{-11}	[*DeMore et al.,* 2000]
$O(^1D) + O_2 \rightarrow O(^3P) + O_2$	4.00×10^{-11}	[*Atkinson et al.,* 2001]
$HONO + OH \rightarrow H_2O + NO_2$	4.50×10^{-12}	[*DeMore et al.,* 1997]
$N_2O_5 + H_2O \rightarrow 2\ HNO_3$	1.99×10^{-12}	[*Atkinson et al.,* 2001]
$N_2O + O(^1D) \rightarrow 2\ NO$	6.70×10^{-11}	[*DeMore et al.,* 2000]
$O(^3P) + O_2 \rightarrow O_3$	1.48×10^{-14}	[*DeMore et al.,* 2000]
$O(^1D) + O_3 \rightarrow 2\ O_2$	1.20×10^{-10}	[*DeMore et al.,* 1997]
$O(^1D) + O_3 \rightarrow 2\ O(^3P) + O_2$	1.20×10^{-10}	[*DeMore et al.,* 1997]
$O(^3P) + O_3 \rightarrow 2\ O_2$	8.00×10^{-15}	[*DeMore et al.,* 1997]
$H + O_2 \rightarrow HO_2$	1.20×10^{-12}	[*DeMore et al.,* 1997]
$O(^1D) + H_2O \rightarrow 2\ OH$	2.20×10^{-10}	[*DeMore et al.,* 1997]
$O(^3P) + H_2O_2 \rightarrow OH + HO_2$	1.70×10^{-15}	[*DeMore et al.,* 1997]
$OH + O_3 \rightarrow HO_2 + O_2$	7.80×10^{-14}	[*DeMore et al.,* 2000]
$2\ OH \rightarrow O(^3P) + H_2O$	1.90×10^{-12}	[*DeMore et al.,* 1997]
$2\ OH \rightarrow H_2O_2$	5.90×10^{-12}	[*DeMore et al.,* 1997]
$OH + HO_2 \rightarrow O_2 + H_2O$	1.10×10^{-10}	[*DeMore et al.,* 2000]
$OH + H_2O_2 \rightarrow HO_2 + H_2O$	1.70×10^{-12}	[*DeMore et al.,* 1997]
$HO_2 + O_3 \rightarrow OH + 2\ O_2$	2.00×10^{-15}	[*DeMore et al.,* 1997]
$O(^3P) + OH \rightarrow O_2 + H$	3.30×10^{-11}	[*DeMore et al.,* 1997]
$H + O_3 \rightarrow OH + O_2$	2.90×10^{-11}	[*DeMore et al.,* 1997]
$O(^3P) + HO_2 \rightarrow OH + O_2$	5.90×10^{-11}	[*DeMore et al.,* 2000]
$OH + HNO_3 \rightarrow H_2O + NO_3$	1.54×10^{-13}	[*DeMore et al.,* 2000]
$2\ HO_2 \rightarrow H_2O_2 + O_2$	1.70×10^{-12}	[*DeMore et al.,* 1997]
$N_2O_4 \rightarrow N_2O_{4(wall)}$	5.00×10^{-02}	Model Fit[b]
$N_2O_{4(wall)} \rightarrow N_2O_4$	1.50×10^{-04}	Model Fit
$N_2O_{4(wall)} + H_2O \rightarrow Asym\text{-}N_2O_{4(wall)} + H_2O$	9.21×10^{-21}	Model Fit
$Asym\text{-}N_2O_{4(wall)} + NO_2 \rightarrow NO_2 + N_2O_{4(wall)}$	4.00×10^{-20}	Model Fit
$Asym\text{-}N_2O_{4(wall)} + H_2O \rightarrow HONO_{(wall)} + HNO_{3(wall)}$	2.00×10^{-22}	Model Fit
$HONO_{(wall)} \rightarrow HONO$	2.00×10^{-1}	Model Fit
$HONO \rightarrow HONO_{(wall)}$	7.50×10^{-2}	Model Fit
$2\ HNO_{3(wall)} \rightarrow NO_2^+ + NO_3^- + H_2O$	2.00×10^{-20}	Model Fit
$NO_2^+ + NO_3^- + HONO_{(wall)} \rightarrow 2\ NO + HNO_{3(wall)}$	5.92×10^{-17}	Model Fit
$HONO_{(wall)} + HNO_{3(wall)} \rightarrow Products$	6.00×10^{-19}	Model Fit
$Products \rightarrow N_2O_{4(wall)}$	3.29×10^{-5}	Model Fit
$NO + HNO_{3(wall)} \rightarrow HONO + NO_2$	6.85×10^{-21}	Model Fit

[a]Termolecular reactions with a third body are accounted for in the rate constants using [M] = 2.46×10^{-19} molecules cm^{-3} to match experimental conditions.
[b]See Text

To determine the extent to which NO_2 hydrolysis was affected by irradiation, the time dependencies of NO_2, NO, and HONO formation were compared to model-predicted concentration time-profiles for these species. These model predictions are generated from a kinetics model created by specifying all the reactions (with their rate constants) known to be occurring in the LPC (Table 1) with the inclusion of several reactions used to simulate the heterogeneous reactions in the NO_2 hydrolysis as per the mechanism suggested by Finlayson-Pitts *et al. (*2002). The gas phase rate constants are from known sources [*Tsang and Herron,* 1991; *DeMore et al.,* 1997; *DeMore et al.,* 2000; *Atkinson et al.,* 2001]. Heterogeneous reactions are not explicitly represented by the model; instead they are represented in terms of a gas phase analog. The heterogeneous reactions were fit in the model to match experimental data over a range of concentrations (20 – 100 ppm NO_2) and relative humidities (20 – 80%). The chemical model software used was REACT v1.2 [*Braun et al.,* 1988; *Bozzelli,* 2000; *Manka,* 2001]; it is a zero-dimensional gas phase model that numerically integrates rate equations for all species over specified time intervals.

To experimentally determine the photolysis rate constants for NO_2 and HONO for use in our kinetics model, NO_2 or HONO was added to the LPC in concentrations similar to those in the NO_2 hydrolysis experiments, and the cell then filled to 1 atm with N_2. Irradiation (300 – 400 nm) began after the cell was filled to 1 atm of N_2 and an initial FTIR spectrum was taken. The concentrations of the gaseous species were then monitored with time by FTIR with the photolysis lamp on. The HONO was generated using a HONO generator, which is described by [*Barney et al.,* 2000], so only a brief description is described herein. In the generator, HONO is produced by passing humid air (80-100% RH) over $NaNO_2$ powder (Aldrich, 99.5%) which was then reacted with gaseous HCl prepared from flowing dry N_2 over 1:10 mixture of HCl (Fisher, 12.1 M) and Nanopure® water:

$$NaNO_{2(s)} + HCl_{(g)} \rightarrow HONO_{(g)} + NaCl_{(s)} \qquad (6)$$

3. RESULTS AND DISCUSSION

Figure 3 shows an NO_2 hydrolysis experiment carried out in the dark for ~7 hr at a relative humidity of 80% and 50 ppm initial NO_2. The NO_2 slowly decays while HONO and NO increase. The experimental data are compared to a model calculation specified by Table 1. There is a relatively good match between the data and model calculation for NO_2 and HONO. In addition, the model data predict that HONO formation is first order with respect to NO_2, in agreement with previous studies [*Sakamaki et al.,* 1983; *Pitts,* 1984; *Svensson et al.,* 1987; *Jenkin and Cox,* 1988; *Perrino et al.,* 1988; *Febo and Perrino,* 1991; *Wiesen et al.,* 1995; *Harrison and Collins,* 1998; *Kleffmann et al.,* 1998]. The model over-predicts NO formation; this is most likely due to

difficulties in quantifying NO by FTIR in these experiments. Water absorbs in the region of 1300 cm^{-1} to 2000 cm^{-1} while NO has overlapping fine rotational lines in the region of 1780 cm^{-1} to 1960 cm^{-1}. Subtraction of this large amount of water from a spectrum with a small amount of NO results in a large uncertainty associated with NO quantification.

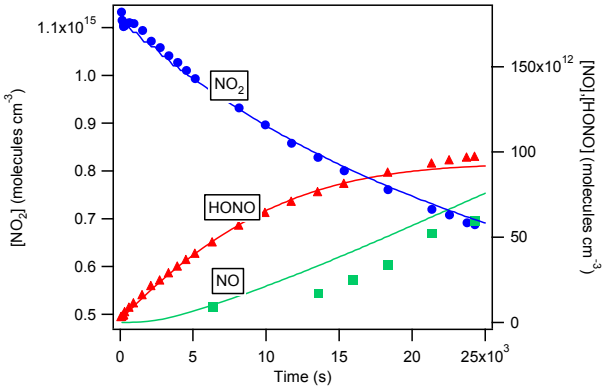

Figure 3. Comparison of experimental data and model-predicted time profiles of NO_2, HONO, and NO in the dark for ~7 hr. Solid lines are the model predictions and the data are represented as points.

In Figure 4, a 50 ppm NO_2 hydrolysis experiment at a relative humidity of 80% is shown. In this experiment for the first ~2 hr the HONO accumulates in the dark. The model specified in Table 1 is in excellent agreement with the experimental HONO and NO_2 data during the

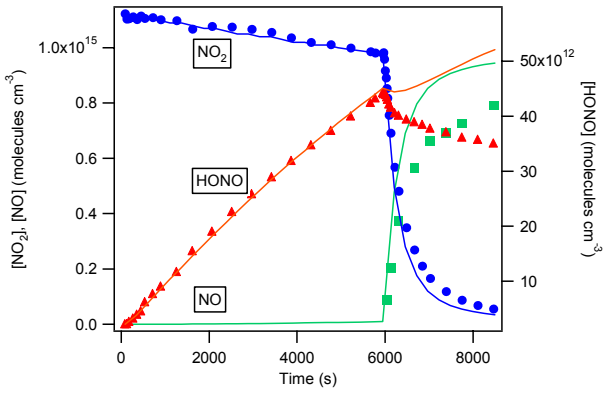

Figure 4. Comparison of experimental data and model-predicted time profiles of NO_2, HONO, and NO. During the first ~6000 s, NO_2 hydrolysis is occurring in the dark. After ~6000 s the radiation begins, i.e., photolysis rate constants are added to the model.

first ~2 hours. Irradiation begins at ~6000 s and continues for the remainder of the experiment. As expected, the NO_2 and HONO photolyze and form a large amount of NO. After 6000 s the model incorporates the HONO and NO_2 photolysis rate constants measured in our cell, (3.5 ± 0.4) x 10^{-4} s^{-1} (2s) and (1.6 ± 0.1) x 10^{-3} s^{-1} (2s) respectively. It can be seen in Figure 4 that, although photolysis of HONO is included in the model, the modeled HONO is predicted to increase after 6000 s, while during the experiment the measured HONO actually decays. This indicates that the HONO formation steps in the model are overestimated in the presence of light. In the experiments of Akimoto et al. (1987), when photolysis began, a photoenhancement of HONO formation was observed, i.e., the experimental HONO data were greater than the model prediction. In our studies, however, the experimental data are far below the model prediction, indicating a "photodepression" of HONO formation.

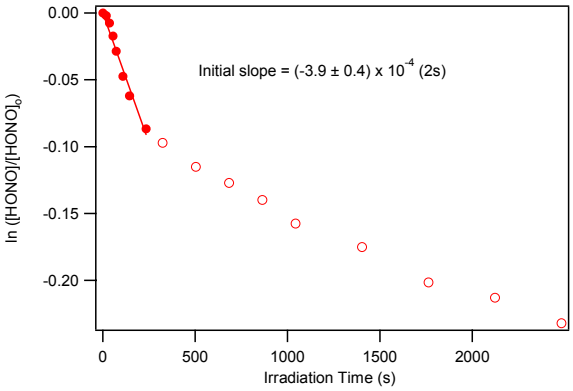

Figure 5. The experimental HONO decay when the lights are turned on is plotted in the form of equation (I). The rate of HONO decay here is very similar to the measured photolysis rate constant of HONO.

Using the first order integrated rate equation (I),

$$\ln\frac{[HONO]}{[HONO]_o} = -kt \qquad (I)$$

the rate constant for experimental HONO decay can be determined and compared to that for photolysis. The

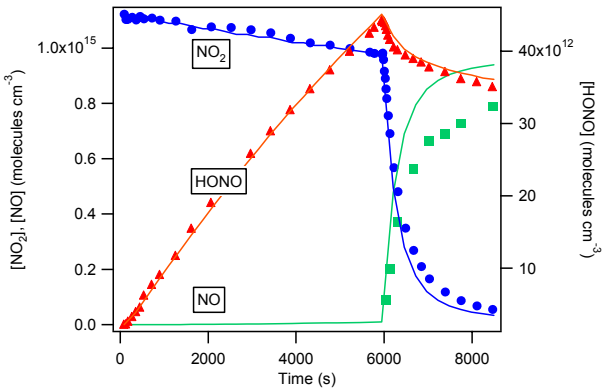

Figure 6. Comparison of experimental data and model-predicted time profiles of NO_2, HONO, and NO. During the first ~6000 s the dark reaction is taking place. After 6000 s the lights are tuned on, the photolysis rate constants are added to the model and the NO_2 hydrolysis mechanism is removed from the model.

initial photolytic decay of HONO in Figure 4 (~6000 – 8000 s) was thus examined more closely in Figure 5 by

plotting $\ln\frac{[HONO]}{[HONO]_o}$ versus irradiation time. The initial slope of this plot resulted in a value of $(3.9 \pm 0.4) \times 10^{-4}$ s^{-1} (2s) for the first order loss of HONO decay during irradiation, which is equal, within experimental error, to the measured HONO photolysis rate constant of $(3.5 \pm 0.4) \times 10^{-4}$ s^{-1} (2s). This suggests that HONO production from NO_2 hydrolysis ceases when irradiated by light in the region of 300 – 400 nm. In Figure 6 this is tested by removing the NO_2 hydrolysis mechanism from the model when the lights are turned on. Excellent agreement is obtained between the experimental data and the model calculation that suggests the NO_2 hydrolysis mechanism proposed is actually deactivated in the presence of 300 – 400 nm light.

Although we do not see the photoenhancement effect that Akimoto *et al.* (1987) observed, the conditions of their experiments differed from ours. First, they used filtered Xe arc lamps which produce a broad range of light from 290 nm through the infrared region while the blacklights used in this study only produce light in the range of 300 nm to 400 nm. Since Akimoto *et al.*, used a broader wavelength region, it is possible that a complex photoenhancement mechanism is occurring outside of our wavelength region and a "photodepression" is occurring in our narrow wavelength region. The second possibility lies in the diluent gas. Akimoto *et al*. used air while we used nitrogen. It is possible that oxygen plays a critical role in the photoenhancement effect of Akimoto *et al*. Work is currently in progress to elucidate these possibilities.

4. ATMOSPHERIC IMPLICATIONS

NO_2 hydrolysis is currently believed to be a major source of HONO in the atmosphere, especially at night when HONO photolysis does not occur. Since HONO photolysis at dawn is a major source of OH radicals, which drive the chemistry of the troposphere, it is important that reaction (1) be accurately included in airshed models to determine its impacts. While current airshed models typically utilize rates of HONO production from previous laboratory studies to represent reaction (1), this may not be appropriate given the complexities of the reaction. As we have shown, the presence of radiation significantly impacts NO_2 hydrolysis possibly by deactivating the reactive species leading to HONO formation. In addition, there may be a multipart mechanism dependent on the wavelengths of radiation present.

However, photochemical HONO formation has been recently reported in field studies [*Zhou et al.,* 2001; *Dibb et al.*, 2002; *Zhou et al.* 2002]. Both Dibb et al. and Zhou et al. (2001) measured photochemical HONO production in the Artic snow exposed to either sunlight or artificial light (λ > 280 nm). Zhou et al. (2002) measured a peculiar formation of HONO while sampling rural air in a glass sampling manifold upon exposure to sunlight. They proposed that HONO was formed by hydrolysis of NO_2, which was generated upon photolysis of nitric acid present on the glass. Currently, this mechanism is unclear, but light does seem to play an important role.

The experiments carried out here were performed in a borosilicate glass long path cell in which the glass walls acted as the support for a thin film of water and other surface species. Water uptake measurements suggest that water films are likely to be present on surfaces typically found in the lower part of the troposphere, such as building materials, soils, and vegetation [*Lammel,* 1999; *Sumner and Finlayson-Pitts,* 2002 (Paper No. 1.4)]. Therefore, there are likely to be similarities in this chemistry and that occurring on thin films in the lower troposphere. This area of **SURFACE** (**S**urfaces, **U**rban, and **R**emote: **F**ilms **A**s a **C**hemical **E**nvironment) may impact the ozone and NO_x chemistry in the troposphere.

5. ACKNOWLEDGEMENTS

We are thankful to the California Air Resources Board (Contract No. 00-323) and the National Science Foundation (Grant No. ATM-0097573) for the support of this work. We would also like to thank J. N. Pitts Jr. and L. M. Wingen for many useful discussions.

6. REFERENCES

Akimoto, H.; Takagi, H.; Sakamaki, F., 1987: Photoenhancement of the Nitrous Acid Formation in the Surface Reaction of Nitrogen Dioxide and Water Vapor. *J. Phys. Chem. A,* **19,** 539-551

Alicke, B.; Platt, U.; Stutz, J., 2002: Impact of Nitrous Acid on the Total Hydroxyl Radical Budget During the LOOP/PIPAPO Study in Milan. *J. Geophys. Res. Atmos,* In Press

Atkinson, R.; Baulch, D. L.; Cox, R. A.; Crowley, J. N.; Hampson, R. F.; Kerr, J. A.; Rossi, M. J.; Troe, J., 2001: Summary of Evaluated Kinetic and Photochemical Data for Atmospheric Chemistry. *IUPAC Subcommittee on Gas Kinetic Data Evaluation for Atmospheric Chemistry,* Chemical Kinetics Data Center, National Institute of Standards and Technology, Gaithersberg, Maryland 20899, USA

Bandow, H.; Akimoto, H.; Akiyama, S.; Tezuka, T., 1984: Photolysis of asym-N_2O_4 ($ONONO_2$) Isolated in an Argon Matrix at 11K. *Chem. Phys. Lett.,* **111,** 496-500

Barney, W. S.; Finlayson-Pitts, B. J., 2000: Enhancement of N_2O_4 on Porous Glass at Room Temperature: A Key Intermediate in the Heterogeneous Hydrolysis of NO_2? *J. Phys. Chem. A,* **104,** 171-175

Barney, W. S.; Wingen, L. M.; Lakin, M. J.; Brauers, T.; Stutz, J.; Finlayson-Pitts, B. J., 2000: Infrared Absorption Cross-section Measurements for Nitrous

Acid (HONO) at Room Temperature. *J. Phys. Chem. A,* **104,** 1692-1699

Barney, W. S.; Wingen, L. M.; Lakin, M. J.; Brauers, T.; Stutz, J.; Finlayson-Pitts, B. J., 2001: Infrared Absorption Cross-section Measurements for Nitrous Acid (HONO) at Room Temperature. *J. Phys. Chem. A,* **105,** 4166

Bozzelli, 2000: REACT for Windows: Chemical Kinetics Emulation and Application. *J. Chem. Educ.,* **77,** 165

Braun, W.; Herron, J.; Kahaner, D., 1988: ACUCHEM: A Computer Program for Modeling Complex Chemical Reaction Systems. *Int. J. Chem. Kinet.,* **20,** 51-62

Caudle, P. G.; Denbigh, K. G., 1953: Kinetics of the Absorption of Nitrogen Pentoxide into Water and Aqueous Solutions. *Trans. Faraday Soc.,* **49,** 39-52

Cheung, J. L.; Li, Y. Q.; Boniface, J.; Shi, Q.; Davidovits, P.; Worsnop, D. R.; Jayne, J. T.; Kolb, C. E., 2000: Heterogeneous Interactions of NO_2 With Aqueous Surfaces. *J. Phys. Chem. A,* **104,** 2655-2662

DeMore, W. B.; Friedl, R. R.; Sander, S. P.; Golden, D. M.; Hampson, R. F.; Howard, C. J.; J., K. M.; Huie, R. E.; Ravishankara, A. R.; Colb, C. E.; Molina, M. J.; Moortgat, G. K., 2000: Chemical Kinetics and Photochemical Data for Use in Stratospheric Modeling, Supplement to Evaluation 12: Update of Key Reactions, Evaluation Number 13. *Jet Propulsion Laboratory, California Institute of Technology, Pasadena, CA,* JPL Publication 00-3

DeMore, W. B.; Sander, S. P.; Golden, D. M.; Hampson, R. F.; Howard, C. J.; J., K. M.; Ravishankara, A. R.; Colb, C. E.; Molina, M. J., 1997: Chemical Kinetics and Photochemical Data for Use in Stratospheric Modeling, Evaluation Number 12. *Jet Propulsion Laboratory, California Institute of Technology, Pasadena, CA,* JPL Publication 97-4

Dibb, J. E.; Arsenault, M.; Peterson, M. C.; Honrath, R. E., 2002: Fast Nitrogen Oxide Photochemistry in Summit, Greenland Snow. *Atmos. Environ.*, **36**, 2501-2511.

England, C.; Corcoran, W., 1974: Kinetics and Gas-Phase Reaction of Water Vapor and Nitrogen Dioxide. *Ind. Eng. Chem.,* **13,** 373-384

Febo, A.; Perrino, C., 1991: Prediction and Experimental Evidence for High Air Concentration of Nitrous Acid in Indoor Environments. *Atmos. Env.,* **25,** 1055-1061

Finlayson-Pitts, B. J.; Pitts, J. N. *Chemistry of the Upper and Lower Atmosphere: Theory, Experiments, and Applications*; Academic Press: San DIego, 2000.

Finlayson-Pitts, B. J.; Wingen, L. M.; Sumner, A. L.; Syomin, D.; Ramazan, K. A., 2002: The Heterogeneous Hydrolysis of NO_2 in Laboratory Systems and in Outdoor and Indoor Atmospheres: An Integrated Mechanism. *Phys. Chem. Chem. Phys,* Submitted

Goodman, A. L.; Bernard, E. T.; Grassian, V. H., 2001: Spectroscopic Study of Nitric Acid and Water Adsorption on Oxide Particles: Enhanced Nitric Acid Uptake Kinetics in the Presence of Adsorbed Water. *J. Phys. Chem. A,* **105,** 6443-6457

Goodman, A. L.; Underwood, G. M.; Grassian, V. H., 1999: Heterogeneous Reaction of NO_2: Characterization of Gas-phase and Adsorbed Products from the Reaction, $2NO_2(g)+H_2O(a)$-> $HONO(g)+HNO_3(a)$ on Hydrated Silica Particles. *J. Phys. Chem. A,* **103,** 7217-7223

Graham, R. F.; Tyler, B. J., 1972: Formation of Nitrous Acid in a Gas-phase Stirred Flow Reactor. *J. Chem. Soc., Faraday Trans. I,* **68,** 683-688

Harrison, R.; Collins, G., 1998: Measurements of Reaction Coefficients of NO_2 and HONO on Aerosol Particles. *J. Atmos. Chem.,* **30,** 397-406

Harrison, R. M.; Peak, J. D.; Collins, G. M., 1996: Tropospheric Cycle of Nitrous Acid. *J. Geophys. Res. Atmos.,* **101,** 14429-14439

Jenkin, M. E.; Cox, R. A., 1988: Laboratory Studies of the Kinetics of Formation of Nitrous Acid from the Thermal Reaction of Nitrogen Dioxide and Water Vapour. *Atmos. Environ.,* **22,** 487-498

Kleffmann, J.; Becker, K. H.; Wiesen, P., 1998: Heterogeneous NO_2 Conversion Processes on Acid Surfaces: Possible Atmospheric Implications. *Atmos. Env.,* **32,** 2721-2729

Lammel, G., 1999: Formation of Nitrous Acid: Parameterization and Comparison with Observations. Max-Planck-Institut-fur Meteorolgie, Report #286.

Lammel, G.; Cape, J., 1996: Nitrous Acid and Nitrite in the Atmosphere. *Chem. Soc. Rev.,* **25,** 361-369

Manka, M. J., 2001: REACT for Windows, Version 1.2. *Alchemy Software,* Wesley Chapel, FL

Mertes, S.; Wahner, A., 1995: Uptake of Nitrogen Dioxide and Nitrous Acid On Aqueous Surfaces. *J. Phys. Chem.,* **99,** 14000-14006

Perner, D.; Platt, U., 1979: Detection of Nitrous Acid in the Atmosphere by Differential Optical Absorption. *Geophys. Res. Lett.,* **6,** 917-920

Perrino, C.; Desantis, F.; Febo, A., 1988: Uptake of Nitrous Acid and Nitrogen Oxides by Nylon Surfaces: Implications for Nitric Acid Measurement. *Atmos. Environ.,* **22,** 1925-1930

Peters, M. S.; Holman, J. L., 1955: Vapor- and Liquid-Phase Reactions between Nitrogen Dioxide and Water. *Ind. Eng. Chem.,* **47,** 2536-2539

Pitts, J. N., Sanhueza, E., Atkinson, R.,Carter, W.,Winer, A., Harris, W., and Plum, C., 1984: An Investigation of the Dark Formation of Nitrous Acid in Environmental Chambers. *Int. J. Chem. Kinet.,* **16,** 919-939

Platt, U.; Perner, D.; Harris, G. W.; Winer, A. M.; Pitts Jr., J. N., 1980: Observations of Nitrous Acid in an Urban Atmosphere by Differential Optical Absorption. *Nature,* **285,** 312-314

Sakamaki, F.; Hatakeyama, S.; Akimoto, H., 1983: Formation of Nitrous Acid and Nitric Oxide in the Heterogeneous Dark Reaction of Nitrogen Dioxide and Water Vapor in a Smog Chamber. *Int. J. Chem. Kin.,* **15,** 1013-1029

Schiller, C.; Locquiao, S.; Johnson, T.; Harris, G., 2001: Atmospheric Measurements of HONO by Tunable Diode Laser Absorption Spectroscopy. *J. Atmos. Chem,* **40,** 275-293

Sumner, A. L. and B. J. Finlayson-Pitts, 2002: Steps Toward Understanding Heterogeneous Chemistry

in the Troposphere: Water Uptake on Environmentally Relevant Surfaces, Paper No. 1.4, American Meteorological Society 83rd Annual Meeting, Long Beach, CA, February 2003.

Stutz, J.; Alicke, B.; Neftel, A., 2002: Nitrous Acid Formation in the Urban Atmosphere: Gradient Measurements of NO_2 over Grass in Milan, Italy. *J. Geophys. Res. Atmos.,* In Press

Svensson, R.; Ljungstrom, E.; Lindqvist, O., 1987: Kinetics of the Reaction between Nitrogen Dioxide and Water Vapor. *Atmos. Environ.,* **21,**

Tsang, W.; Herron, J. T., 1991: Chemical Kinetic Data Base for Propellant Combustion I. Reactions Involving NO, NO_2, HNO, HNO_2, HCN, and N_2O. *J. Phys. Chem. Ref. Data,* **20,** 609-663

Wayne, L. G.; Yost, D. M., 1952: Kinetics of Rapid Gas Phase Reaction between NO, NO_2, and H_2O. *J. Chem. Phys,* **19,** 41-47

White, J. U., 1942: Long Optical Paths of Large Aperture. *J. Opt. Soc. Am.,* **32,** 285-288

Wiesen, P.; Kleffmann, J.; Kurtenbach, R.; Becker, K., 1995: Mechanistic Study of the Heterogeneous Conversion of NO_2 into HONO and N_2O on Acid Surfaces. *Faraday Discuss,* 121-127

Wingen, L. M., A. L. Sumner, D. Syomin, K. A. Ramazan, B. J. Finlayson-Pitts, 2002: Heterogeneous Formation of Nitrous Acid in Laboratory Systems, Paper No. P1.8, American Meteorological Society 83rd Annual Meeting, Long Beach, CA, February 2003

Winer, A. M.; Biermann, H. W., 1994: Long Pathlength Differential Optical Absorption Spectroscopy (DOAS) Measurements of Gaseous HONO, NO_2, and HCHO in the California South Coast Air Basin. *Res. Chem. Intermed.,* **20,** 423-445

Zhou, X.; Beine, H. J.; Honrath, R. E.; Fuentes, J. D.; Simpson, W.; Shepson, P. B.; Bottenheim, J. W., 2001: Snowpack Photochemical Production of HONO: a Major Source of OH in the Arctic Boundary Layer in Springtime. *Geophys. Res. Lett.*, **28**, 4087-4090.

Zhou, X.; He, Y.; Huang, G.; Thornberry, T.; Carroll, M.; Bertman, S., 2002: Photochemical Production of Nitrous Acid on Glass Manifold Surface. *Geophys. Res. Lett.,* In Press

.